Antarctic Science 24(2), 183–192 (2012) © Antarctic Science Ltd 2011 doi:10.1017/S0954102011000745

Evaluation of Antarctic Mesoscale Prediction System (AMPS) cyclone forecasts using infrared satellite imagery

MELISSA A. NIGRO, JOHN J. CASSANO and SHELLEY L. KNUTH

Department of Atmospheric and Oceanic Sciences, Co-operative Institute for Research in Environmental Sciences, University of Colorado, 216 UCB, Boulder, CO 80309, USA
melissa.nigro@colorado.edu

Abstract: The Antarctic coast is an area of high cyclonic activity. Specifically, the regions of Terra Nova Bay, in the western Ross Sea, and Byrd Glacier, in the western Ross Ice Shelf, are prone to cyclone development. The United States, New Zealand, and Italian Antarctic programmes conduct extensive research activities in the region of the western Ross Sea. Due to the harsh weather conditions associated with the cyclonic systems that occur in this region and the abundant research activities in the area, it is important to be able to accurately predict the timing, location and strength of cyclones in this sector of Antarctica. This study evaluates the ability of the Antarctic Mesoscale Prediction System (from 2006–09) to accurately forecast cyclones in the region of the western Ross Sea by comparing the Antarctic Mesoscale Prediction System forecasts to cyclones identified in infrared satellite imagery. The results indicate that the Antarctic Mesoscale Prediction System is able to accurately predict the presence of cyclones about 40% of the time (at a minimum) and the presence of no cyclones about 70% of the time.

Received 13 April 2011, accepted 24 August 2011, first published online 17 October 2011

Key words: cyclone forecasting, model evaluation, remote sensing, Ross Sea sector, Weather Research and Forecasting (WRF) model

Introduction

The Southern Hemisphere is a region of high cyclonic activity. Previous studies indicate that the circumpolar trough, around 60°S, is the region of maximum cyclonic activity in the Southern Hemisphere (Lamb & Britton 1955, Jones & Simmonds 1993, Simmonds & Keay 2000, Simmonds *et al*. 2003, Uotila *et al*. 2009). These studies also discuss the elevated levels of cyclonic activity found in the areas surrounding the Antarctic coastline. Specifically, each of the studies identifies the region surrounding the Ross Sea and the Ross Ice Shelf (RIS) (Fig. 1) as an area of enhanced cyclonic activity. The RIS region is prone to the presence of cyclones due to a combination of local forcing enhanced by regional synoptic patterns (Bromwich 1991, Carrasco & Bromwich 1993, Carrasco & Bromwich 1994, Bromwich *et al*. 2003, Carrasco *et al*. 2003). Typically, a wavenumber three pattern present in the 500 mb geopotential height field surrounds the Antarctic continent (Mo & White 1985, Cai *et al*. 1999), with an upper level trough and coincident cut-off low situated over the Ross Sea and RIS regions. Corresponding to the upper level low, a surface low pressure minimum is located in the eastern Ross Sea (Parish *et al*. 2006). These features induce southerly flow on the western edge of the RIS that can extend over the western portions of the Ross Sea. Southerly flow from the RIS generates cold air advection across areas of the Ross Sea, where relatively warm maritime air interacts with the colder air from the continent to produce a baroclinic zone, which enhances cyclogenesis. Sea ice-free regions of the Ross Sea area, such as within the Terra Nova Bay (Fig. 1) or RIS polynyas, will enhance the development of cyclones by providing a warm, moist convective layer that will further strengthen the baroclinic zone (Bromwich 1991, Carrasco & Bromwich 1994). The strengthening of the baroclinic zone not only enhances cyclogenesis in this region, but also, enhances the strength of the cyclones moving through this region.

The interaction of synoptic-scale systems with small-scale features, such as katabatic winds or local topography, can also work to enhance cyclonic activity in the region of the RIS. For example, on the RIS, decaying synoptic systems that enter the region from the adjacent Ross Sea or West Antarctica can induce warm air advection in the area. The interaction of the warm air with cold air from coastal katabatic flow or southerly winds can produce additional baroclinic zones and induce mesocyclone development over the RIS. An example of this scenario is presented by King & Turner (1997, pp. 209–213) in the case study of "A major weather system crossing West Antarctica, 24–26 May 1988." Additionally, the interaction of large-scale flow with local topography can also induce cyclonic activity in the region of the RIS. For example, it is typical for southerly flow to promote the creation of shear vortices, or von Karman vortices, in the lee of Ross Island (Fig. 1) (Powers *et al*. 2003, Bromwich *et al*. 2005). Although the von Karman vortices are not true mesoscale cyclones, the shear in the flow creates cyclonic and anti-cyclonic features on the

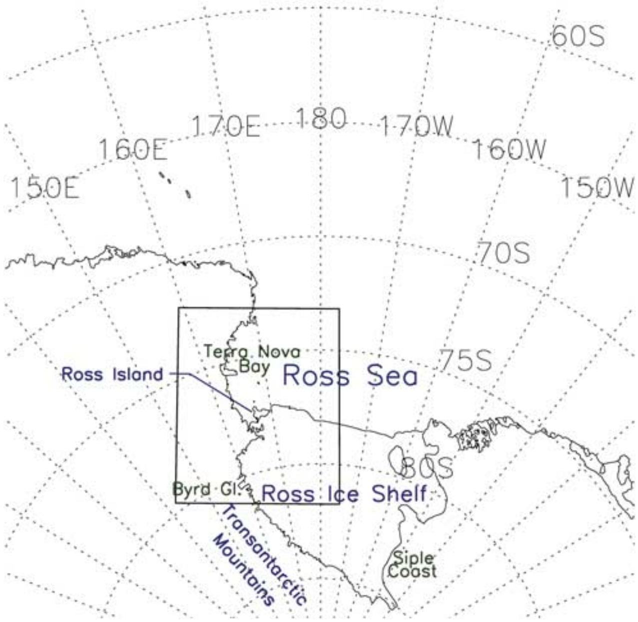

Fig. 1. Map of the Ross Sea region. The black box indicates the Antarctic Mesoscale Prediction System (AMPS) domain three.

western and eastern sides of Ross Island, respectively. It is hypothesized that these vortices have the potential to develop into larger systems.

Previous research has studied the Ross Sea region to determine the frequency of cyclone occurrence. For example, Bromwich (1991) used a combination of automatic weather station observations and satellite images from the Defense Meteorological Satellite Program to determine the frequency of cyclones in the Terra Nova Bay and Byrd Glacier regions (Fig. 1). The study concluded that during the years of 1984 and 1985 approximately one to two cyclones formed per week in the Terra Nova Bay region and about half that number was observed in the area of Byrd Glacier. The conclusions from this study were further supported by a follow-up study conducted by Carrasco & Bromwich (1994). The follow-up study used the same datasets and methods to analyse the cyclones for 1988. The results were in agreement with the previous study, showing that on average about two (one) cyclones developed per week in the Terra Nova Bay (Byrd Glacier) region.

In addition to climatological studies, the development of cyclones in these regions has been investigated on a case study basis. Carrasco & Bromwich (1993) studied the development of four cyclones in the Terra Nova Bay region. The study analysed the contribution of an upper level trough in creating the baroclinic zone. Forcing from the upper level trough enhanced the surface cyclonic circulation advecting maritime air against the coastline, causing it to mix with cold, dry continental air masses. Three of the four cyclones analysed were created by the advection of warm, moist air towards the coast by the upper level forcing. The fourth cyclone was induced by a baroclinic zone formed from the presence of cold, dry continental air transported from the continental interior by katabatic winds and warm, moist maritime air masses found over the open waters of the Terra Nova Bay polynya. The study concluded that in addition to the importance of katabatic drainage and a source of maritime air masses, the region of Terra Nova Bay is especially prone to cyclonic activity due to the semi-permanent upper level trough that is located in this region. It is the combination of these features (katabatic drainage, the availability of maritime air masses and upper level synoptic forcing) that causes specific locations to be more prone to cyclonic activity than others.

The enhanced presence of cyclones in the region of the Ross Sea and the RIS is important to study because of the impact of these cyclones on the weather surrounding Ross Island and McMurdo Station, the largest of the United States Antarctic Program's (USAP) Antarctic bases. For instance, the 15–16 May 2004 McMurdo windstorm caused wind speeds of 35–50 m s^{-1} to be observed at McMurdo Station for a six hour duration. The maximum wind speed observed at McMurdo during this storm was 71.5 m s^{-1} (Steinhoff *et al.* 2008). Due to the intense wind speed and structural damage that occurred at McMurdo Station, Steinhoff *et al.* (2008) used the Antarctic Mesoscale Prediction System (AMPS) to analyse the dynamics of this storm. The case study determined that the high wind event was caused by the development of a cyclone near Siple Coast (Fig. 1). The cyclone traversed the RIS towards the north-west causing a barrier wind to develop along the Transantarctic Mountains (Fig. 1). This strong barrier wind, with speeds of 20–30 m s^{-1}, passed over Minna Bluff and Black Island (Steinhoff *et al.* 2008, fig. 1c) creating a down-slope windstorm that resulted in the very strong winds observed at McMurdo. Given the extensive logistical activities that occur at McMurdo Station it is important to be able to accurately predict the timing, location and intensity of the cyclonic storms that occur frequently in this region.

Antarctic Mesoscale Prediction System is the primary numerical weather prediction (NWP) system used by USAP weather forecasters. The ability of AMPS to simulate a mesoscale cyclone event that occurred from 13–17 January 2001 was investigated by Bromwich *et al.* (2003). This study analysed the 10 km forecasts from the polar-modified version of the MM5 model run within AMPS. Observations from automatic weather stations, ships and satellite imagery indicate the presence of two cyclones in the McMurdo area during this case study, while AMPS simulations indicate only one cyclone. The cyclone predicted by AMPS initially aligned with the more northerly observed cyclone and throughout the period of the case study shifted to track with the more southerly observed cyclone. The model predicted a lower minimum central pressure of the cyclone than either of the observed cyclones. Variations to the initial conditions were found to alter the accuracy of the cyclone forecast, with the position of the upper level forcing and surface low pressure system being most critical.

In March 2006, a version of AMPS based on the Weather Research and Forecasting (WRF) model was introduced and run in parallel with the MM5 version of AMPS. From March 2006–June 2009 both versions of the AMPS output were archived. Starting in July 2009, the MM5 version of AMPS was terminated and only the WRF version of AMPS was run and archived (as of publication). Therefore, it is important to understand the ability of the WRF model within AMPS to predict the presence, timing and location of cyclones in this region. This study will compare cyclones forecast by AMPS during September 2006, 2007, 2008 and 2009 in the western Ross Sea with cyclones identified in corresponding infrared satellite images. This evaluation will determine the skill of AMPS (from 2006–09) in forecasting cyclones in the region surrounding McMurdo Station. The analysis was done for the month of September to coincide with a climatological study of the Terra Nova Bay region (Knuth & Cassano 2011) conducted in support of a field campaign that occurred during September 2009 (Cassano *et al*. 2010).

Data

Model

Antarctic Mesoscale Prediction System is a NWP system that has been optimized for use in the Antarctic (Powers *et al*. 2003). The most recent version of AMPS is based on a version of WRF that has been modified for use in the Polar Regions (Hines & Bromwich 2008, Bromwich *et al*. 2009, Hines *et al*. 2011). The most significant changes made to WRF include the implementation of a scheme to treat fractional sea ice, improved treatment of heat transfer through ice and snow surfaces, a revised surface energy balance calculation, and selection of model physics options that are appropriate for polar applications.

The AMPS system was originally developed to provide high-resolution, polar specific forecasts over Antarctica in support of USAP operations. Antarctic Mesoscale Prediction System is currently run by the National Center for Atmospheric Research (NCAR) as an experimental real-time NWP system and is used by the USAP and other national Antarctic programmes. This study uses archived output from twice-daily AMPS simulations for Septembers from 2006–09. The first guess initial and lateral boundary conditions for AMPS come from the National Centers for Environmental Prediction (NCEP) 0.5 degree Global Forecast System (GFS) model output. Observations are assimilated into AMPS using the WRF three dimensional variational data assimilation capability. Information on the WRF configuration and physics packages used in the operational version of AMPS can be found in Powers (2007) and on the AMPS website at http://www.mmm.ucar.edu/rt/wrf/amps/.

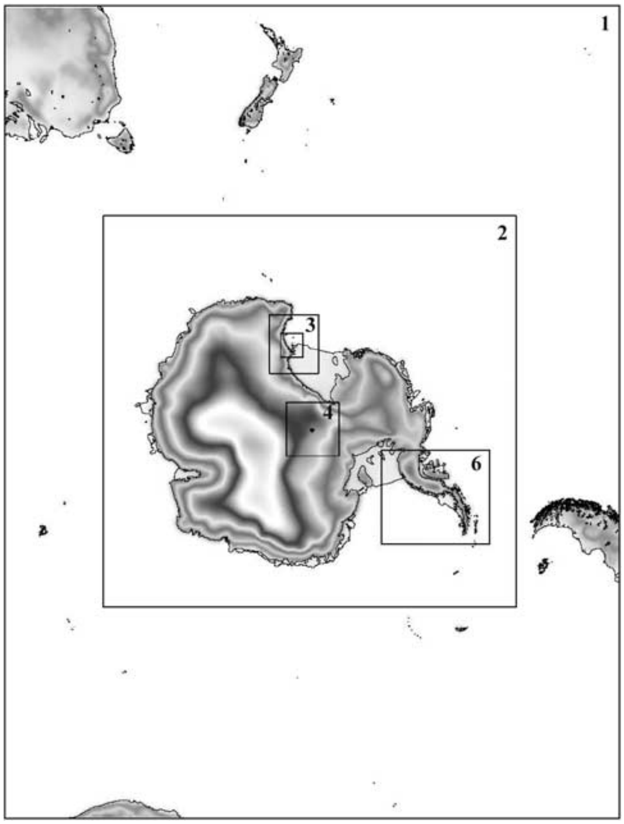

Fig. 2. Map of Antarctic Mesoscale Prediction System (AMPS) domains. Domains one, two, three, four and six are labelled in the upper right corner of the respective outlined box. Domain five is located within the outline of domain three and is represented by an unlabelled box. Figure courtesy of the National Center for Atmospheric Research, Mesoscale and Microscale Meteorology Division, http:/www.mmm.ucar.edu/rt/wrf/amps/information/configuration/maps.html, accessed August 2011.

It is important to note that AMPS is not a static system. Continuous improvements are made to the system and therefore the configuration of AMPS is constantly evolving. Consequently, the results of the model evaluation presented in this paper are valid for the AMPS configuration for the Septembers from 2006–09. Although these results are limited in time, the results will be important for research conducted using AMPS output and for future improvements made to the system. Additionally, the results will provide a snapshot of the ability of AMPS (a major NWP system for the Antarctic) to forecast high impact weather systems.

During the period of this analysis, 2006–09, the version of the WRF model run within AMPS was upgraded. From March 2006–November 2008 the WRFV2.2 version of WRF was used within AMPS. From November 2008–April 2011 the WRFV3.0.1.1 version of WRF was used within AMPS. The WRF model within AMPS uses terrain following vertical co-ordinates with 44 full eta-levels. The model is run

https://doi.org/10.1017/S0954102011000745 Published online by Cambridge University Press

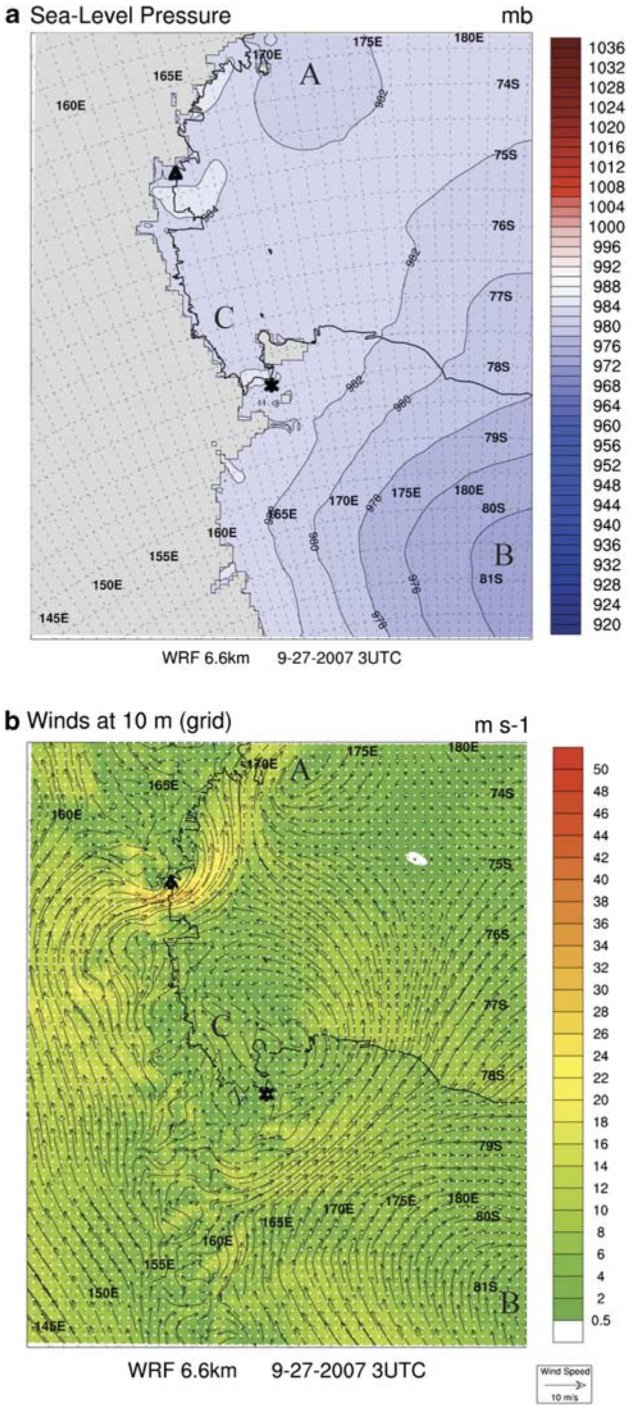

Fig. 3. a. Antarctic Mesoscale Prediction System sea level pressure, and **b.** 10-metre winds from 03 UTC 27 September 2007. In a. point A shows a closed sea level pressure contour, point B shows a curved sea level pressure contour, and point C shows no local minima in the sea level pressure field. In b. point A shows a closed cyclonic circulation, point B shows a possible closed cyclonic circulation that is partially outside the model domain, and point C shows a not fully closed cyclonic circulation.

with a set of six two-way interactively nested domains with horizontal grid spacing of 60 km, 20 km, 6.7 km, 6.7 km, 2.2 km and 6.7 km from March 2006–November 2008 and 45 km, 15 km, 5 km, 5 km, 1.67 km and 5 km from November 2008 to the time of publication (see Fig. 2). Forecasts for the western Ross Sea AMPS domain three (6.7 or 5 km horizontal grid spacing) are used in this study. This domain includes the areas of active mesoscale cyclogenesis near Terra Nova Bay and the north-western RIS. Forecasts for domain three are run for 36 hours with the output archived every hour. The sea level pressure (SLP) and 10-metre winds (the winds at ten metres above the surface) from the 12–23 hour forecasts were used to identify cyclones in the AMPS output.

Satellite

Satellite infrared images were used to evaluate the cyclones forecast by AMPS. The infrared images were created from the local area coverage (LAC) data from the National Oceanic and Atmospheric Administration (NOAA)-18 and NOAA-19 satellites. The LAC data is available from the Advanced Very High-resolution Radiometer (AVHRR) instrument and has a resolution of 1 km. This resolution is higher than the resolution of the AMPS domain and therefore is sufficient to evaluate the AMPS forecasts. The satellite data was retrieved from the Antarctic Meteorological Research Center at the University of Wisconsin-Madison (adde://amrc.ssec.wisc.edu, accessed April 2009). On average approximately one satellite image of the Ross Sea region was available per day. For the duration of the four months used for this study, 16 days had no images available and 14 days had more than one image available. Every available image during Septembers from 2006–09 was used for this study.

Methods

Model

Model output from the 12–23 hour forecasts was used to create plots of the SLP and the 10-metre winds (Fig. 3). Sea level pressure values were not plotted for elevations > 500 m due to the large errors that occur when calculating SLP in the Antarctic for high elevation locations. The SLP plots (with a 2 mb contour interval) were analysed for the presence of curved or closed contours around minima in the SLP field (see points A and B in Fig. 3a), indicating the presence of a low pressure system. Additionally, the 10-metre wind plots were analysed for the presence of a closed cyclonic circulation or cyclonically curved winds that would indicate a closed cyclonic circulation near the edge of the domain (see points A and B in Fig. 3b). To identify the presence of a cyclone in the AMPS output, it was required that evidence of a cyclone was shown in both

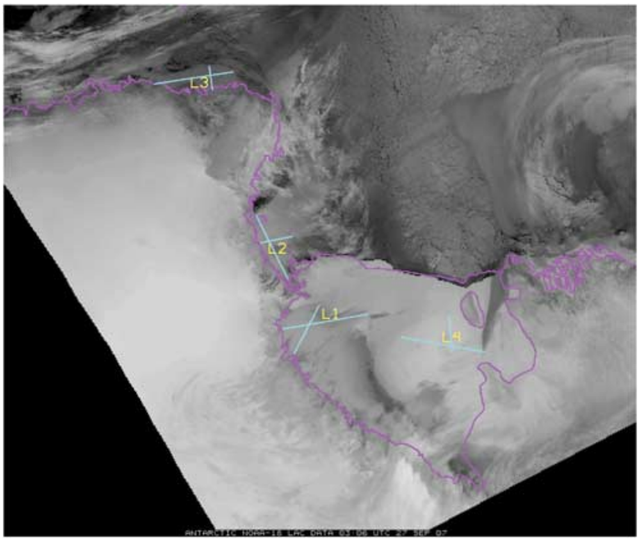

Fig. 4. Infrared satellite image from 0306 UTC 27 September 2007. Labels L1, L2, L3 and L4 indicate the centre of identified cyclones and the lines indicate the dimensions of the identified cyclones.

the SLP and 10-metre wind plots. For each identified cyclone, the centre latitude and longitude, the minimum central pressure and the maximum wind speed were recorded. It was also noted if a closed SLP contour enclosed the cyclone. In order to categorize the size of the cyclone as synoptic-scale or mesoscale, the shortest and longest diameter across the cyclonic circulation were measured (Turner *et al*. 1998). This was done using the 10-metre wind plots because the edge of the cyclonic signature was more clearly defined in these plots. The long diameter was used to group the cyclones into synoptic-scale (≥ 1000 km) and mesoscale (< 1000 km) categories.

Satellite

Cyclones were identified by manual analysis of satellite images centred on 74°S, 175°W (Fig. 4), and were classified by size, shape, and location, using criteria defined in previous studies (Carleton & Fitch 1993, Turner *et al*. 1998, Carrasco *et al*. 2003). The size of each system was found by measuring the shortest and longest portions of the cyclone (Turner *et al*. 1998). The size of each system was also characterized by mesoscale or synoptic-scale using the same method as described above (Heinemann 1990, Bromwich 1991, Carrasco *et al*. 2003).

It is important to note that there are limitations in using satellite infrared imagery to determine the presence of cyclones in a given region. Specifically, it is possible for the satellite image to falsely indicate the presence of no cyclones when a cyclone is actually present. There are two scenarios in which this commonly occurs. The first scenario occurs when upper level clouds mask the low level features in the satellite image. In this scenario, the cloud signature associated with a surface cyclone would not be evident in the satellite image and therefore missed during the analysis. The second scenario occurs when a cyclone does not contain a cloud signature. Carrasco & Bromwich (1994) determined that cloud-free mesoscale cyclones occur in the region of the RIS during the winter months. When this occurs the satellite image lacks the cloud signature necessary for cyclone identification. Due to these limitations in identifying cyclones in infrared satellite imagery, the statistics provided for the ability of AMPS to correctly forecast the presence of a cyclone will be presented as a minimum. Essentially, AMPS could correctly forecast a cyclone that is not observed in the satellite imagery and it would falsely be categorized as an incorrect forecast.

Verification

The dates and times used for the comparison of the AMPS forecasts to the infrared satellite images were determined by the availability of satellite images. For each available satellite image during Septembers from 2006–09 the corresponding AMPS output was retrieved to the nearest hour. The cyclones identified in the satellite images were compared to the cyclones identified in the AMPS output. The cyclones were grouped into three categories: 1) cyclones that were identified in both the satellite image and the AMPS output and were located within 300 km of each other and had a similar size and shape in both datasets, 2) cyclones that were observed in the satellite image and not identified in the AMPS output, and 3) cyclones that were identified in the AMPS output and not observed in the satellite image. For instance, referring to Figs 3 & 4 it can be seen that the cyclone indicated by point B in the AMPS output is an accurate prediction of the L4 cyclone in the satellite image. Therefore, this cyclone was grouped into category one. The L1 cyclone identified in the satellite image (Fig. 4) was not forecast by AMPS, which is shown by the lack of a SLP minima and the lack of a cyclonic signature in the winds for this location in Fig. 3. Therefore this cyclone was classified as a category two cyclone. The L2 cyclone in Fig. 4 was also grouped into category two. This cyclone is slightly misleading because its location matches the cyclonic flow at point C in the AMPS 10-metre wind output. Although, by carefully analysing the AMPS output it can be seen that the flow at point C, as shown by the AMPS 10-metre winds, does not show a fully closed cyclonic circulation and, more importantly, the AMPS output does not indicate a minima in the SLP field at this location. Therefore, the AMPS output does not meet the criteria for cyclone identification and the L2 cyclone is grouped into category two. Lastly, the cyclone identified by point A in the AMPS output is not observed in the satellite image and was classified as a category three cyclone.

https://doi.org/10.1017/S0954102011000745 Published online by Cambridge University Press

It should also be noted that the domain of the satellite images is larger than the domain of the AMPS output. Only the cyclones identified in the satellite images that were within the AMPS domain were analysed. Therefore, the L3 cyclone in Fig. 4 was not included in the study. If the centre of the cyclone identified in the satellite images was outside of the AMPS domain, it was included in the study if the cyclonic flow, or curved winds, could be observed within the AMPS domain (for example, the combination of point B in Fig. 3 and L4 in Fig. 4).

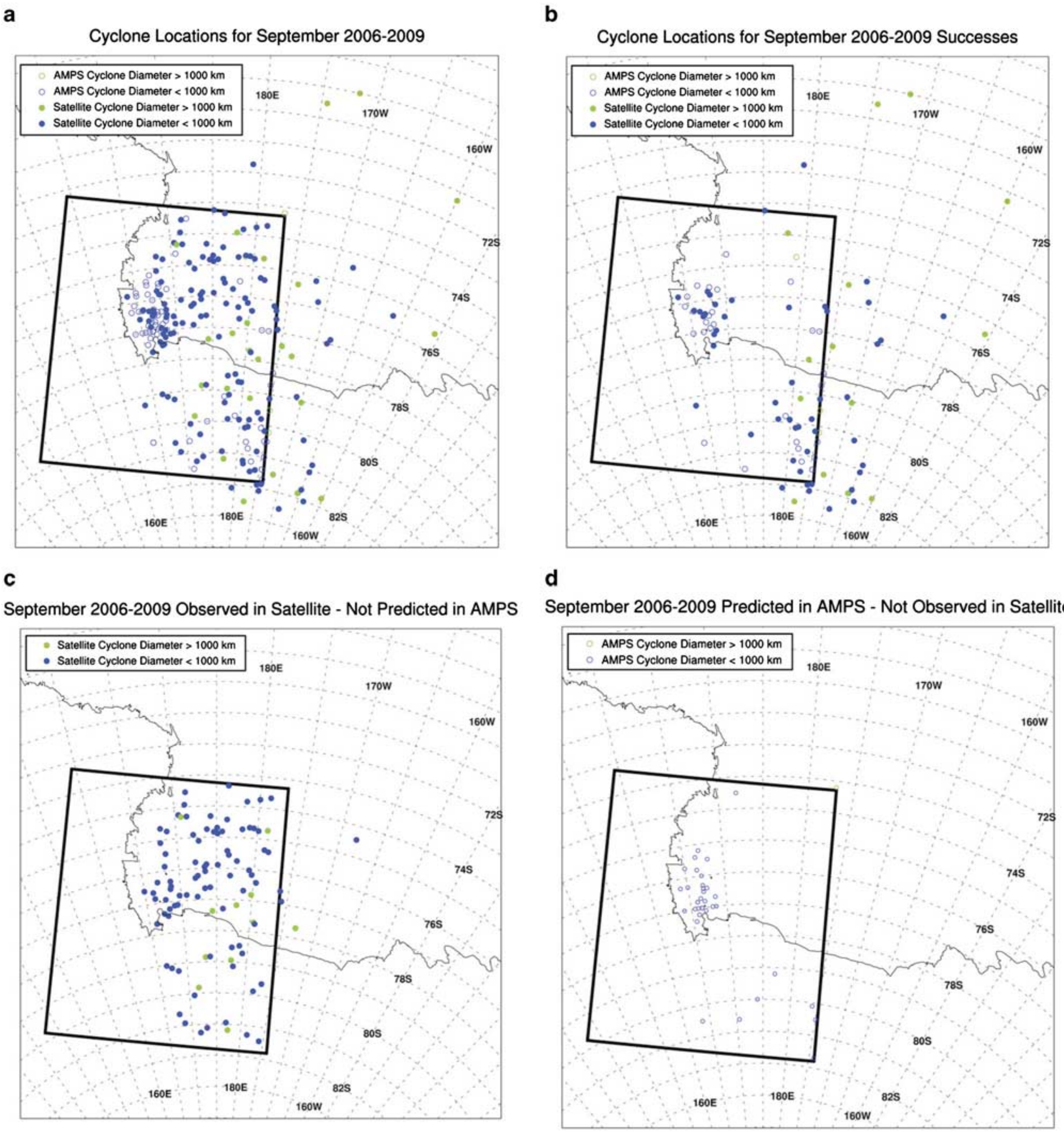

Fig. 5. Location of Antarctic Mesoscale Prediction System (AMPS) (hollow circles) and satellite (solid circles) identified cyclones. **a.** Shows all of the AMPS and satellite identified cyclones, **b.** shows the category one cyclones (cyclones identified in both the AMPS and satellite images), **c.** shows all of the category two cyclones (only identified in the satellite images), and **d.** shows all the category three cyclones (only identified in AMPS). In each panel blue circles indicate mesocyclones and the green circles indicate synoptic-scale cyclones.

https://doi.org/10.1017/S0954102011000745 Published online by Cambridge University Press

Results and discussion

During Septembers from 2006–09, a total of 123 satellite images (27 in 2006, 28 in 2007, 35 in 2008, and 33 in 2009) were available. Each satellite image was analysed for the presence of cyclones, resulting in the identification of a total of 159 cyclones. From a comparison (to the nearest hour) of these cyclones to the AMPS identified cyclones, it was determined that AMPS forecast 63 of these cyclones (40% of total cyclones observed in the satellite images). If only the requirement for a maximum distance of 300 km between cyclone centres was used, and the size and shape criteria were neglected, AMPS forecast 67 (42%) of the cyclones observed in the satellite images. As previously mentioned, these statistics indicate the minimum number of correctly forecast cyclones by AMPS for this period. Additionally, out of the 123 total images, 33 satellite images indicated no presence of a cyclone within the domain of interest. A direct comparison of these images to the AMPS plots indicated that AMPS correctly forecast no cyclones for 23 of these images (70% of the satellite images with no cyclones present). Conversely, during this time frame AMPS predicted a total of 37 cyclones that were not observed in the satellite images. Due to limitations in identifying cyclones in satellite images, this represents the maximum number of falsely predicted AMPS cyclones. The remainder of this section will further investigate and discuss these results.

Figure 5 shows the spatial distribution of the cyclones identified in this study. Solid circles show cyclones identified from the satellite images, while hollow circles show cyclones identified from the AMPS data. In the figure the blue circles identify mesocyclones and the green circles identify synoptic cyclones. Figure 5a shows all cyclones identified within the AMPS output and the satellite imagery. Several points are illustrated in this figure. First, matching previous studies discussed in the introduction, clusters of observed and forecast cyclones are shown in the Terra Nova Bay region and to the north of Ross Island. Additionally, more mesoscale cyclones than synoptic-scale cyclones were identified throughout the entire domain. This is potentially due to both the location and the limited area of the domain chosen. Extratropical cyclones tend to intensify as the systems approach the circumpolar trough from the north (Jones & Simmonds 1993). Subsequently, as the synoptic systems move through the trough and continue to travel towards the south the cyclones typically begin to decay (Lamb & Britton 1955, Jones & Simmonds 1993, Simmonds & Keay 2000, Simmonds *et al.* 2003, Uotila *et al.* 2009). This results in a decreased number of synoptic-scale cyclones in the region surrounding the Antarctic continent. Conversely, the greater number of mesocyclones within the area of this study is probably due to the presence of coastal baroclinic zones within the Terra Nova Bay region and along the Transantarctic Mountains, as well as, the topographically generated cyclones on the northern edge of Ross Island.

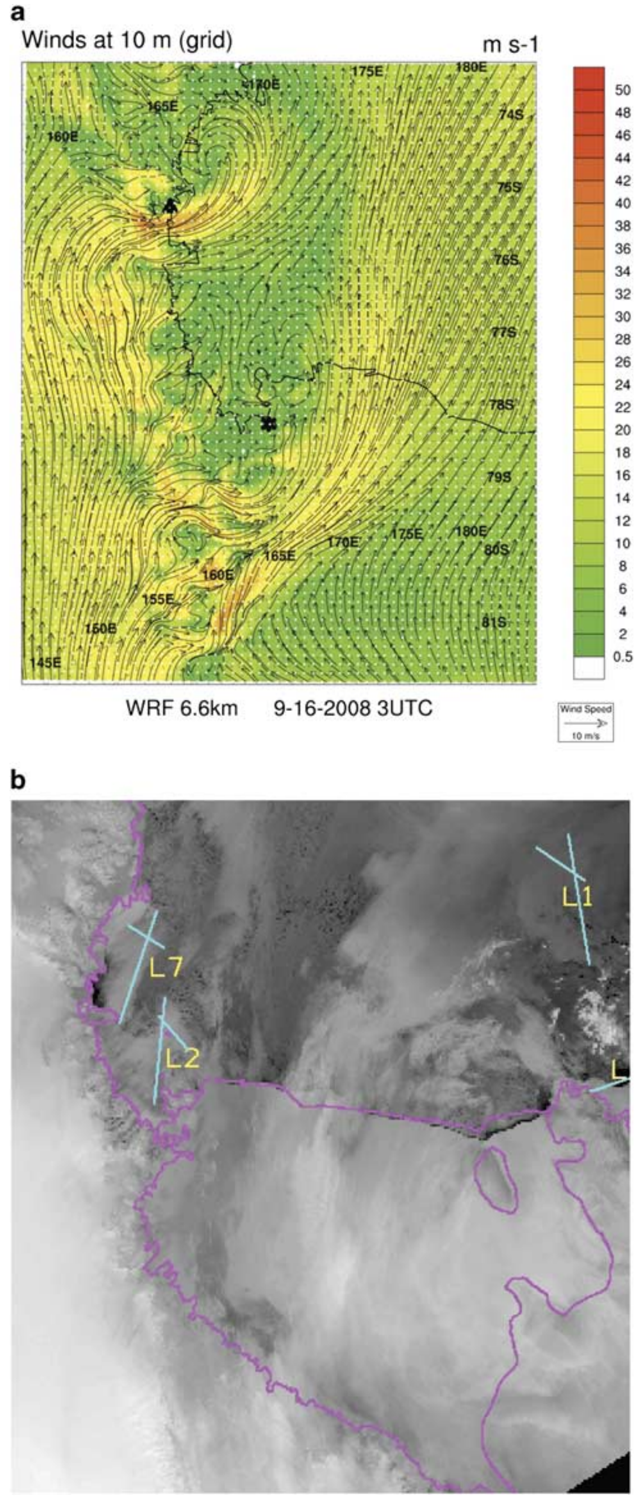

Fig. 6. a. Antarctic Mesoscale Prediction System 10-metre winds at 03 UTC 16 September 2008, and **b.** infrared satellite image at 3:28 UTC 16 September 2008.

Figure 5b shows the cyclones that were identified in the satellite images and were forecast in the AMPS output (category one). These results show that there are several

https://doi.org/10.1017/S0954102011000745 Published online by Cambridge University Press

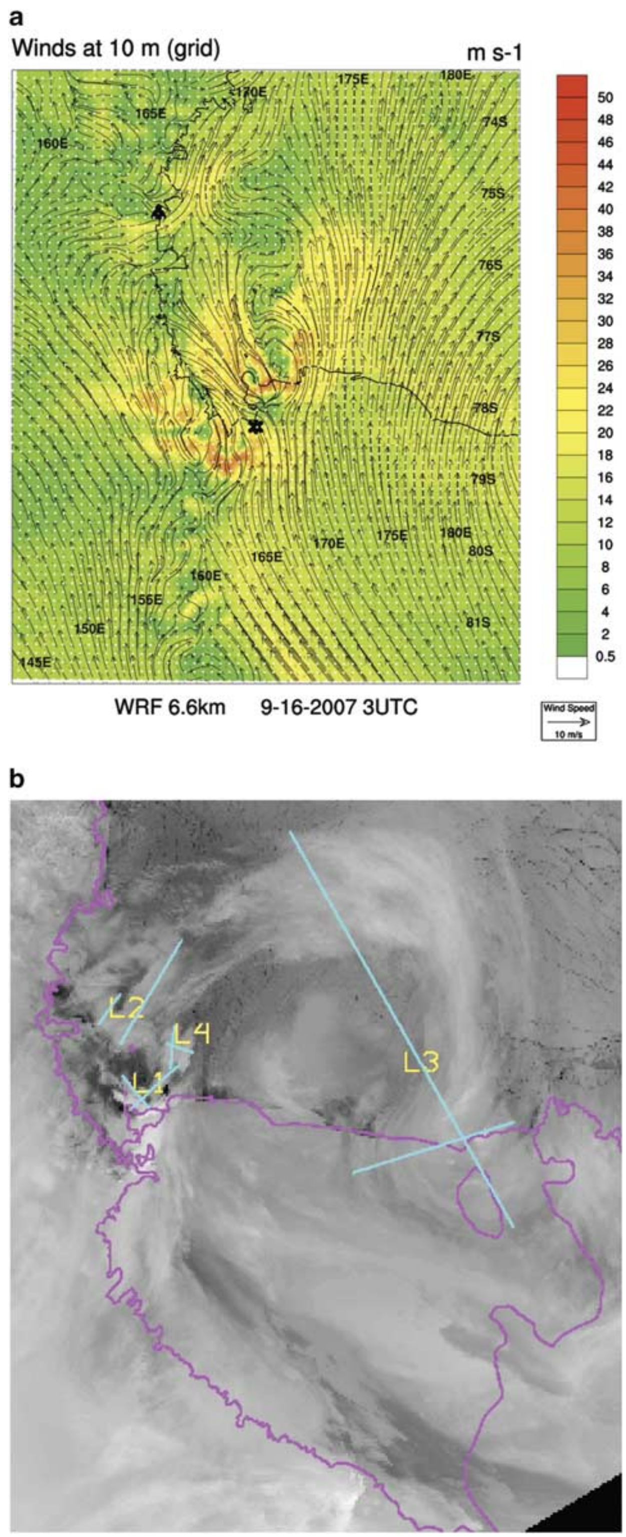

Fig. 7. a. Antarctic Mesoscale Prediction System 10-metre winds at 03 UTC 16 September 2007, and **b.** infrared satellite image at 3:19 UTC 16 September 2007. The cyclones observed in the lee of Ross Island are labelled in b.

instances when AMPS correctly predicts mesoscale cyclones to the north of Ross Island. It has been hypothesized that these vortices may be von Karman vortices that develop due to the shear created as air flows past a large protruding topographic obstacle, in this case Ross Island, in the presence of a temperature inversion (Powers *et al.* 2003, Bromwich *et al.* 2005). Although these systems are not true mesocyclones, it is hypothesized that they have the ability to develop into larger systems north of Ross Island. Figure 5b also indicates that AMPS is successful at predicting the cyclonic systems in the eastern portion of the domain. The topography in this area is less complex than the topography in the western portion of this domain and may contribute to the ability of AMPS to more accurately forecast cyclones for this region. Uotilia *et al.* (2009) found that the ability of AMPS to forecast cyclones identified in reanalyses decreased in the vicinity of sharp topographic changes. This is consistent with the ability of AMPS to more accurately predict the presence of cyclones in the relatively flat eastern portion of the domain than in the western portion of the domain in the vicinity of the Transantarctic Mountains. For the cyclones that were correctly forecast by AMPS, the average distance between the centre latitude and longitude of the satellite observed cyclone and the AMPS forecast cyclone was 126 km, with a minimum distance of 23 km and a maximum distance of 288 km. Given the size of these cyclones and the maximum 30 min time difference between the satellite image and the AMPS forecast, this was considered to represent fairly accurate predictions of the cyclone locations.

Figure 5c shows the cyclones that were identified in the satellite images, but were not forecast by AMPS (category two). This panel shows a wide range of cyclones over the area of the domain that were not forecast by AMPS. When comparing Fig. 5c to Fig. 5b it can be seen that AMPS often fails to predict the cyclones in the western Ross Sea. Each of these cyclones was analysed. The results indicate that for approximately half of these cyclones, the AMPS output was dominated by other flow features. For example, the L7 cyclone in Fig. 6b is not forecast by the AMPS output (Fig. 6a). In this case, the AMPS output shows a strong katabatic wind event. The katabatic winds predicted by the model indicate shear vorticity and the development of anti-cyclonic flow, not cyclonic flow. In other instances, strong southerly flow off of the RIS dominated the region of interest. In these instances, it appears that AMPS is either incorrectly forecasting the dominant flow feature or is unable to forecast the small cyclonic circulation in the presence of other strong forcing (strong katabatic or synoptic flow).

The results also indicate that there are instances where AMPS fails to predict the von Karman vortices in the lee of Ross Island. In these instances the AMPS 10-metre winds often show strongly perturbed flow in the lee of Ross Island (see Fig. 7a). Within the perturbed flow there is some cyclonic turning, but no closed cyclonic circulation. Without the presence of a closed cyclonic circulation, the system did not fit the criteria for cyclone identification in this study. It is possible that the open cyclonic circulation could be responsible for generating the cloud signature identified in the satellite images. Of the 22 satellite identified cyclones north of Ross Island not identified in the AMPS output, there were 11 instances where the AMPS output showed cyclonically perturbed flow in this region.

Cyclones forecast by AMPS but not identified in the satellite images (category three cyclones) are shown in Fig. 5d. Due to limitations in identifying cyclones in satellite images, such as upper level cloud cover and cloud-free cyclones, this represents the maximum number of falsely predicted AMPS cyclones. Figure 5d indicates that the majority of the cyclones in category three are mesocyclones located to the north of Ross Island. In this region, the von Karman vortices are low level features that can easily be masked by upper level clouds in the satellite images. Additionally, these cyclones are small and could potentially be associated with weak forcing. Therefore, in some cases these systems may lack a cloud signature and therefore be difficult to identify on the satellite images. Conversely, this may indicate that AMPS over predicts shear induced cyclone formation to the north of Ross Island. Future research on von Karman vortices in the lee of Ross Island will be necessary in order to better understand these features and the ability of AMPS to correctly forecast the presence of these systems.

Conclusion

In this study, the cyclone forecasts from the WRF model within AMPS (from 2006–09) were evaluated using infrared satellite imagery. Each satellite image that was available during Septembers 2006–09 was analysed for the presence of a cyclone in the western Ross Sea region and compared to the AMPS forecast for the same period. The results indicate that, at a minimum, AMPS was able to correctly forecast 40% of the cyclones identified in the analysis. Additionally, AMPS was able to correctly predict the presence of no cyclones 70% of the time. The results indicated that the majority of the cyclones observed in the region were mesocyclones, with the northern edge of the domain located too far south to capture the presence of synoptic-scale cyclones associated with the circumpolar trough. It was determined that AMPS is able to predict the cyclones in the eastern portion of the domain, away from the complex topography of the Transantarctic Mountains, with greater accuracy than the western portion of the domain. This is in agreement with previous studies on the ability of AMPS to forecast mesocyclones in the region of the Transantarctic Mountains. Additionally, it was determined that AMPS occasionally misses the prediction of smaller systems due to the influence of the large-scale flow in the region. For example, the katabatic drainage in the region of Terra Nova Bay can dominate the AMPS forecast, preventing the accurate prediction of mesocyclones in this region. The use of a higher resolution domain in this region could potentially alleviate some of these errors. Lastly, it was determined that the ability of AMPS to forecast the von Karman vortices that spin up due to shear in the lee of Ross Island is quite variable. The identification of these systems dominated the cyclone climatology in this region. It was discussed that both the identification and prediction of these systems is difficult due to the fact that the von Karman vortices are a low level feature that are associated with severely perturbed flow. Additional research and observations of the von Karman vortices in the lee of Ross Island could lead to improved forecasting of these systems in the future.

Acknowledgements

The AMPS data was retrieved courtesy of the National Center for Atmospheric Research-Computational and Information Systems Laboratory. The authors appreciate the support of Matthew Lazzara and the Antarctic Meteorological Research Center at the University of Wisconsin-Madison for providing the NOAA-18 and NOAA-19 LAC datasets under the NSF grant number ANT-0838834. This research was supported by NSF grants ANT 0636811, ANT 0739464 and ATM 0404790. The constructive comments of the reviewers are also gratefully acknowledged.

References

Bromwich, D.H. 1991. Mesoscale cyclogenesis over the southwestern Ross Sea linked to strong katabatic winds. *Monthly Weather Review*, **119**, 1736–1753.

Bromwich, D.H., Hines, K.M. & Bai, L.-S. 2009. Development and testing of polar Weather Research and Forecasting model: 2. Arctic Ocean. *Journal of Geophysical Research*, **114**, 10.1029/2008JD010300.

Bromwich, D.H., Monaghan, A.J., Manning, K.W. & Powers, J.G. 2005. Real-time forecasting for the Antarctic: an evaluation of the Antarctic Mesoscale Prediction System (AMPS). *Monthly Weather Review*, **133**, 579–603.

Bromwich, D.H., Monaghan, A.J., Powers, J.G., Cassano, J.J., Wei, H., Kuo, Y.K. & Pellegrini, A. 2003. Antarctic Mesoscale Prediction System (AMPS): a case study from the 2000–01 field season. *Monthly Weather Review*, **131**, 412–434.

Cai, W., Baines, P.G. & Gordon, H.B. 1999. Southern mid- to high latitude variability, a zonal Wavenumber-3 pattern, and the Antarctic Circumpolar Wave in the CSIRO coupled model. *Journal of Climate*, **12**, 3087–3104.

Carleton, A.M. & Fitch, M. 1993. Synoptic aspects of Antarctic mesocyclones. *Journal of Geophysical Research*, **98**, 12 997–13 018.

Carrasco, J.F. & Bromwich, D.H. 1993. Mesoscale cyclogenesis dynamics over the southwestern Ross Sea, Antarctica. *Journal of Geophysical Research*, **98**, 12 973–12 995.

Carrasco, J.F. & Bromwich, D.H. 1994. Climatological aspects of mesoscale cyclogenesis over the Ross Sea and Ross Ice Shelf regions of Antarctica. *Monthly Weather Review*, **122**, 2405–2425.

Carrasco, J.F., Bromwich, D.H. & Monaghan, A.J. 2003. Distribution and characteristics of mesoscale cyclones in the Antarctic: Ross Sea eastward to the Weddell Sea. *Monthly Weather Review*, **131**, 289–301.

Cassano, J.J., Maslanik, J.A., Zappa, C.J., Gordon, A.L., Cullather, R.I. & Knuth, S.L. 2010. Observations of Antarctic polynya with unmanned aircraft systems. *EOS Transactions*, **91**, 245, 10.1029/2010EO280001.

Heinemann, G. 1990. Mesoscale vortices in the Weddell Sea region (Antarctica). *Monthly Weather Review*, **118**, 779–793.

Hines, K.M. & Bromwich, D.H. 2008. Development and testing of polar Weather Research and Forecasting (WRF) model. Part I: Greenland ice sheet meteorology. *Monthly Weather Review*, **136**, 1971–1989.

Hines, K.M., Bromwich, D.H., Bai, L.-S., Barlage, M. & Slater, A.G. 2011. Development and testing of polar WRF. Part III. Arctic land. *Journal of Climate*, **24**, 26–48.

Jones, D.A. & Simmonds, I. 1993. A climatology of Southern Hemisphere extratropical cyclones. *Climate Dynamics*, **9**, 131–145.

King, J.C. & Turner, J. 1997. *Antarctic meteorology and climatology*. Cambridge: Cambridge University Press, 409 pp.

Knuth, S.L. & Cassano, J.J. 2011. An analysis of near-surface winds, air temperature, and cyclone activity in Terra Nova Bay Antarctica from 1993–2009. *Journal of Applied Meteorology and Climatology*, **50**, 660–682.

Lamb, H.H. & Britton, G.P. 1955. General atmospheric circulation and weather variations in the Antarctic. *The Geographical Journal*, **121**, 334–349.

Mo, K.C. & White, G.H. 1985. Teleconnections in the Southern Hemisphere. *Monthly Weather Review*, **113**, 22–37.

Parish, T.R., Cassano, J.J. & Seefeldt, M.W. 2006. Characteristics of the Ross Ice Shelf air stream as depicted in Antarctic Mesoscale Prediction System simulations. *Journal of Geophysical Research*, **111**, 10.1029/2005JD006185.

Powers, J.G. 2007. Numerical prediction of an Antarctic severe wind event with the Weather Research and Forecasting (WRF) Model. *Monthly Weather Review*, **135**, 3134–3157.

Powers, J.G., Monaghan, A.J., Cayette, A.M., Bromwich, D.H., Kuo, Y. & Manning, K.W. 2003. Real-time mesoscale modeling over Antarctica: the Antarctic Mesoscale Prediction System. *Bulletin of the American Meteorological Society*, **84**, 1533–1545.

Simmonds, I. & Keay, K. 2000. Mean Southern Hemisphere extratropical cyclone behaviour in the 40-year NCEP-NCAR reanalysis. *Journal of Climate*, **13**, 873–885.

Simmonds, I., Keay, K. & Lim, E. 2003. Synoptic activity in the seas around Antarctica. *Monthly Weather Review*, **131**, 272–288.

Steinhoff, D.F., Bromwich, D.H., Lamberston, M., Knuth, S.L. & Lazzara, M.A. 2008. A dynamical investigation of the May 2004 McMurdo Antarctica severe wind event using AMPS. *Monthly Weather Review*, **136**, 7–26.

Turner, J.T., Marshall, G.J. & Lachlan-Cope, T.A. 1998. Analysis of synoptic-scale low pressure systems within the Antarctic Peninsula sector of the circumpolar trough. *International Journal of Climatology*, **18**, 253–280.

Uotila, P., Pezza, A.B., Cassano, J.J., Keay, K. & Lynch, A.H. 2009. A comparison of low pressure system statistics derived from a high-resolution NWP output and three reanalysis products over the Southern Ocean. *Journal of Geophysical Research*, **114**, 10.1029/2008JD011583.